Journal of Alloys and Compounds 778 (2019) 756–760

Contents lists available at ScienceDirect

Journal of Alloys and Compounds

journal homepage: http://www.elsevier.com/locate/jalcom

Low temperature thermodynamics of Yb_6MoO_{12} and Lu_6MoO_{12}

K. Denisova [a], A. Shlyakhtina [b], O. Yumashev [c], M. Avdeev [d], M. Abdel-Hafiez [e, f, g], O. Volkova [a, g, h], A. Vasiliev [a, g, i, *]

[a] Lomonosov Moscow State University, Moscow, 119991, Russia
[b] Semenov Institute of Chemical Physics, RAS, Moscow, 119991, Russia
[c] Institute of Applied Mechanics, RAS, Moscow, 125040, Russia
[d] Australian Nucl Sci & Technol Org, NSW, 2232, Australia
[e] Harvard University, Cambridge, MA, 02138, USA
[f] Center High Pressure Sci & Technol Adv Res, Beijing, 100094, China
[g] National University of Science and Technology "MISiS", Moscow, 119049, Russia
[h] Ural Federal University, Ekaterinburg, 620002, Russia
[i] National Research South Ural State University, Chelyabinsk, 454080, Russia

ARTICLE INFO

Article history:
Received 20 September 2018
Received in revised form
11 November 2018
Accepted 13 November 2018
Available online 17 November 2018

Keywords:
Magnetism
Low temperature
New compounds

ABSTRACT

We report on thermodynamic properties of both rhombohedral $R\bar{3}$ and cubic $Ia\bar{3}$ phases of $Yb_6MoO_{12-\delta}$ supplemented by measurements of $Lu_6MoO_{12-\delta}(R\bar{3})$ magnetic properties. Among these series, $Yb_6MoO_{12-\delta}(R\bar{3})$ only exhibits signatures of magnetic long-range order at T_N~2.5 K which is confirmed by both physical property measurements and neutron powder diffraction. Low temperature specific heat measured down to 100 mK suggests the rearrangement of magnetic subsystem at $T^* = 500$ mK.

1. Introduction

The rare earth molybdenum oxides attract attention as luminescent materials, effective catalysts and ion conductors. The useful features of Yb – Mo – O system stem from the combination of ytterbium ions phosphor property [1] and molybdenum ions ability to exhibit multiple oxidation and valence states. The chemistry of ytterbium – molybdenum oxides is quite rich. Similarly impressive is the diversity of crystal structure types realized in these compounds. Tetravalent molybdenum is met in Yb_2MoO_5 (space group $P2_1/c$) [2], $Yb_2Mo_2O_7$ ($Fd\bar{3}m$) [3] and $Yb_4Mo_5O_{16}$ ($Fd\bar{3}m$) [4]. Pentavalent molybdenum forms $YbMoO_4$ [5] and Yb_3MoO_7 [6]. The family of ytterbium molybdates is constituted by four compounds of hexavalent molybdenum Yb_2MoO_6 ($C2/c$) [7], $Yb_2Mo_4O_{15}$ ($P2_1/c$) [8], Yb_6MoO_{12} ($R\bar{3}$) [9] and $Yb_6Mo_2O_{15}$ ($P3$) [10]. Besides, there are so called metal cluster compounds $Yb_4Mo_4O_{11}$ ($P2_1/m$) [11], $Yb_4Mo_{18}O_{32}$ [12] and $YbMo_{16}O_{44}$ ($R\bar{3}$) [13].

Within this multitude, only $Yb_2Mo_2O_7$ and $Yb_4Mo_4O_{11}$ were investigated with respect to basic thermodynamic properties at low temperatures. The magnetism in these compounds is due to the presence of Yb^{3+} ions while Mo^{6+} ions carry no magnetic moment. The pyrochlore $Yb_2Mo_2O_7$ has evidenced the bulk spin-glass behaviour below 17.5 K consistent with some disorder and random distribution of local magnetic fields acting on ytterbium ions [3]. $Yb_4Mo_4O_{11}$ comprised of infinite chains of *trans*-edge-sharing MoO_6 octahedra presents no signatures of magnetic ordering down to 2 K. No information on low temperature thermal properties is available for any ytterbium – molybdenum oxide.

Heavy rare-earth Ln_6MoO_{12} oxides may crystalline in two different defect fluorite structures, i.e. cubic $Ia\bar{3}$ and rhombohedral $R\bar{3}$ modifications [14]. Here, we present the comprehensive investigation of magnetization M and specific heat C_p in Yb_6MoO_{12} ($R\bar{3}$) and primary characterization of Yb_6MoO_{12} ($Ia\bar{3}$) magnetic properties. These results are supplemented by study of magnetization and specific heat in the reference compound, i.e. rhombohedral polymorph of Lu_6MoO_{12}. The crystal structures of both $R\bar{3}$ and $Ia\bar{3}$ polymorphs of Ln_6MoO_{12} are shown in Fig. 1.

Here, we present the results on low temperature thermodynamics and powder neutron scattering on selected members of vast

* Corresponding author. Lomonosov Moscow State University, Moscow, 119991, Russia.
E-mail address: vasil@mig.phys.msu.ru (A. Vasiliev).

https://doi.org/10.1016/j.jallcom.2018.11.158
0925-8388/

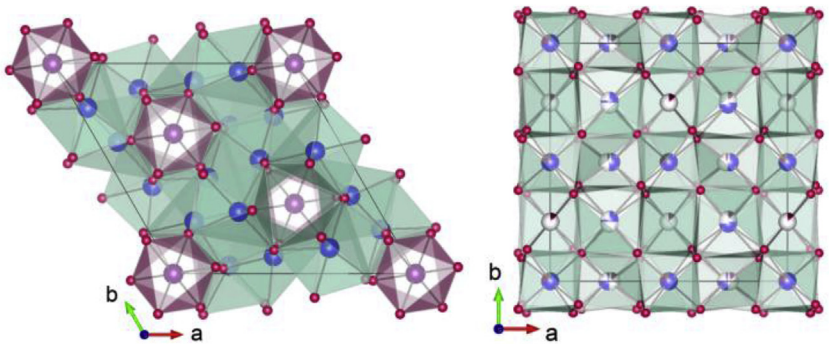

Fig. 1. The crystal structures of $R\bar{3}$ (left) and $Ia\bar{3}$ (right) polymorphs of Ln_6MoO_{12} in polyhedral representation [15].

Ln_6MoO_{12} family of compounds, both rhombohedral and cubic. Among these series, only $Yb_6MoO_{12-\delta}(R\bar{3})$ evidences signatures of the long range magnetic order at low temperatures. The results of systematic study of thermodynamic properties of Ln_6MoO_{12} will be published elsewhere.

2. Methods

The Ln_6MoO_{12} (Ln = Yb, Lu) materials were prepared using the mechanical activation of starting oxides followed by high-temperature heat treatment. All of the rare-earth oxides and molybdenum oxide used in our preparations were of 99.9% purity. After preheating the starting Ln_2O_3 (Ln = Yb, Lu) oxides at 1000 °C for 2 h, they were mixed with the MoO_3 and co-milled in the SPEX8000 ball mill for 1 h. MoO_3 was previously activated in the high energy Aronov ball mill for 4 min. The mechanically activated mixtures of the oxides were pressed at 680 MPa and sintered at 1400 °C or 1600 °C for 3 h. Ln_6MoO_{12} compounds have been furnace −cooled at a rate no greater than 130 °C/h. Lower temperature synthesis provided the rhombohedral $R\bar{3}$ phase. The synthesis at higher temperatures resulted in cubic $Ia\bar{3}$ phase for Yb_6MoO_{12} only. At the same time, Lu_6MoO_{12} seems to undergo a rhombohedral ($R\bar{3}$, no. 148) - bixbyite ($Ia\bar{3}$, no 206) transition at higher temperatures as evidenced by the fact that, in the range 1400–1600 °C, Lu_6MoO_{12} retains the rhombohedral structure [14].

At room temperature, the stable form for both Yb_6MoO_{12} and Lu_6MoO_{12} is an oxygen-ordered rhombohedral modification. We confirm it using the neutron powder diffraction (NPD). NPD data for Yb_6MoO_{12} and Lu_6MoO_{12} samples were collected on the high-resolution neutron powder diffractometer Echidna (OPAL research reactor, Australia) and successfully analyzed using Rietveld method as implemented in the GSAS code. The results are illustrated in Fig. 2 which shows an example of the $Yb_6MoO_{12-\delta}$. The results of NPD data analysis and crystal structural information are presented in Table 1.

Magnetic properties, i.e. in-phase ac - susceptibility χ', dc - susceptibility χ and magnetization M have been investigated in the range 2–300 K up to 9 T using relevant options of "Quantum Design" Physical Properties Measurements System PPMS − 9T. ac − susceptibility measurements were performed for several frequencies in the range 10^3–10^4 Hz with modulation field amplitude 10 G.

Specific heat C_p measurements down to 2 K have been carried out using PPMS with the adiabatic thermal relaxation technique. Specific heat measurements down to 100 mK were performed using a heat-pulse technique within a dilution refrigerator. The addenda value has been measured first and then subtracted from the total specific heat. Thus, the specific heat reported here is only the heat capacity of the sample.

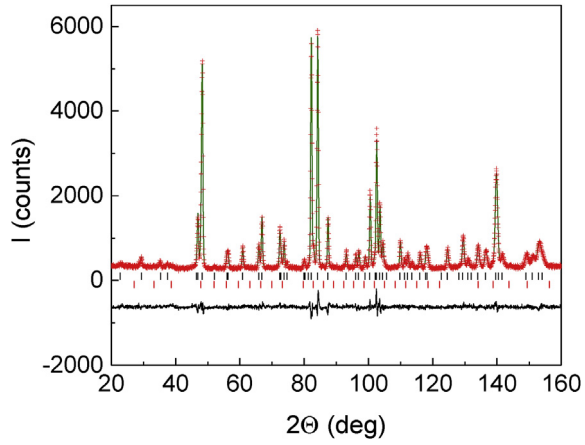

Fig. 2. The Rietveld plot for $R\bar{3}$ polymorph of $Yb_6MoO_{12-\delta}$ based on room temperature NPD data. The two rows of tick marks show the position of peaks for the $Yb_6MoO_{12-\delta}$ and 5.7(4) wt. % Yb_2O_3.

Table 1
Crystal structure data for $Yb_6MoO_{12-\delta}$. and $Lu_6MoO_{12-\delta}$ based on room temperature NPD data. Space group $R\bar{3}$. Ln, Mo, O1, and O2 atoms are located in 18f(x,y,z), 3a(0,0,0), 18f(x,y,z), and 18(x,y,z), respectively.

	$Yb_6MoO_{12-\delta}$	$Lu_6MoO_{12-\delta}$
a, Å	9.63122(14)	9.6182(8)
c, Å	9.18662(18)	9.1482(11)
x(Ln)	0.12069(17)	0.1237(20)
y(Ln)	0.41290(15)	0.4329(15)
z(Ln)	0.02177(14)	0.0208(17)
x(O1)	0.1857(3)	0.184(3)
y(O1)	0.0389(4)	0.023(4)
z(O1)	0.1127(4)	0.111(3)
occupancy(O1)	0.880(1)[a]	1(-)
x(O2)	0.1387(5)	0.1405(17)
y(O2)	0.4436(3)	0.4576(14)
z(O2)	0.2682(3)	0.2627(13)
occupancy(O2)	0.939(1)[*]	0.881(1)[b]
R_p, %	4.90	6.01
R_{wp}, %	6.37	7.80

[a] Refined under a soft restraint of total content of 10.9 per formula unit as determined from magnetic measurements.
[b] Refined under a soft restraint on total content of 11.55 per formula unit as determined from magnetic measurements.

3. Results and discussions

Formally, Lu_6MoO_{12} ($R\bar{3}$) contains no magnetically active ions

and should display the diamagnetic response. However, this compound evidences the paramagnetic behaviour which could be ascribed to the deviation from the oxygen stoichiometry. The results of dc - susceptibility measurements are shown in Fig. 3. The fitting of $\chi(T)$ curve by Curie-Weiss law

$$\chi = \chi_0 + \frac{C}{T - \Theta}$$

in the range 150 – 300 K results in the temperature-independent term $\chi_0 = -\ 7.0 \times 10^{-4}$ emu/mol, the Curie constant $C = 0.34$ emu/molK and the Weiss temperature $\Theta = -\ 145$ K. The value of χ_0 exceeds the diamagnetic correction, i.e. the sum Σ of individual ions Pascal's constants $\chi_\Sigma = -\ 2.5 \times 10^{-4}$ emu/mol [16] which can be attributed to the side effect of the sample holder. The value of C through the definition of effective paramagnetic moment

$$\mu_{eff}^2 = 8C = ng^2S(S+1)$$

determines the number n of magnetically active centres per formula unit with g-factor g and spin-only moment S. Assuming the reduction state of molybdenum Mo^{5+}, with $g = 2$ and $S = 1/2$ one estimates $n = 0.9$ which leads to the specific chemical formula $Lu_6MoO_{11.55}$ or $Lu_6MoO_{12-\delta}$, $\delta = 0.45$. Alternatively, the chemical formula can be written $Lu_6^{3+}Mo_{0.9}^{5+}Mo_{0.1}^{6+}O_{11.55}$. Large negative value of Weiss temperature Θ points to the predominance of antiferromagnetic exchange interactions at elevated temperatures. Tentatively the main couplings are the antiferromagnetic $Mo^{5+} - O - Mo^{5+}$ superexchange and the ferromagnetic $Mo^{5+} - O - Mo^{6+}$ double exchange. The stochastic distribution of magnetically active centres and competition of various couplings may lead to the absence of long range magnetic order down to 2 K.

The magnetic susceptibility χ of Yb_6MoO_{12} ($R\bar{3}$) largely exceeds that of lutetium counterpart due to the abundance of Yb^{3+} magnetic moments, $J = 7/2$, $g = 8/7$. As shown in Fig. 3, at elevated temperatures the $\chi(T)$ dependence follows the Curie-Weiss law with fitting parameters $\chi_0 = 9.3 \times 10^{-3}$ emu/mol, $\Theta = -16$ K and $C = 9.75$ emu/molK. Large positive value of the temperature-independent term χ_0 reflects paramagnetic van Vleck contribution associated with the crystal field splitting of Yb^{3+} ions ground multiplet $^2F_{7/2}$ [17]. Low value of the Weiss temperature as compared to that of Lu_6MoO_{12} rules out presence of appreciable magnetic moment on molybdenum ions. The value of C defines $n = 3.8$ which results in specific chemical formula $Yb_6MoO_{10.9}$ or $Yb_6MoO_{12-\delta}$, $\delta = 1.1$. Alternatively, the chemical formula can be written $Yb_{3.8}^{3}Yb_{2.2}^{2+}Mo^{6+}O_{10.9}$.

At low temperatures, $Yb_6MoO_{12-\delta}$ ($R\bar{3}$) reaches the long range magnetic order. The inset to Fig. 3 shows the temperature dependences of the in-phase part of ac magnetic susceptibility χ′. The position of the broadened peak at T_N ~2.5 K does not depend of the frequency in the range $10^3 \div 10^4$ Hz, thus excluding possible relaxation phenomena. The field dependences of magnetization measured both below and above T_N are shown in Fig. 4. At $T < T_N$, the $M(B)$ curve evidences the behaviour typical for an antiferromagnet, i.e sequence of spin-flop and spin-flip transitions. The spin-flop field $B_{SF} = 2.6$ T. This field is defined by position of broad maximum in dM/dB vs. B curve, as shown in the inset to Fig. 4. Note, that no such anomaly is seen at $T > T_N$. The spin-flip field cannot be defined unambiguously since the temperature of measurement (2 K) is too close to the Neel temperature. As compared to $Yb_6MoO_{12-\delta}$ ($R\bar{3}$) the magnetization of $Lu_6MoO_{12-\delta}$ ($R\bar{3}$) is negligibly small.

The transition into magnetically ordered state in $Yb_6MoO_{12-\delta}$ ($R\bar{3}$) is further confirmed by specific heat measurements. The temperature dependence of Cp is shown in Fig. 5. This curve evidences peak at T_N ~2.5 K and low temperature kink at $T^* = 0.5$ K, as shown in upper inset to Fig. 5. An external magnetic field $B = 9$ T rapidly suppresses the anomaly at Neel temperature resulting in broad anomaly shifted to high temperatures. The Zeeman splitting of $^2F_{7/2}$ multiplet levels is responsible for this Schottky-type anomaly. The specific heat of $Lu_6MoO_{12-\delta}$ ($R\bar{3}$) evidences no features in the temperature range studied. The C_p vs. T curve in Lu compound can be used as a reference for C_p vs. T curve in Yb compound. The simple subtraction of reference data allows roughly estimating the magnetic entropy S_m released in $Yb_6MoO_{12-\delta}$ ($R\bar{3}$). The temperature dependence of this entity is shown in lower inset to Fig. 5. The value obtained $S_m = 43$ J/molK is about two third of expected for specific chemical formula $Yb_{3.8}^{3+}Yb_{2.2}^{2+}Mo^{6+}O_{10.9}$. Note, that the procedure of subtraction of the reference compound data is not straightforward since Lu and Yb compounds evidence different deviations from stoichiometry. That is why, contrary to expectations, the specific heat in Lu compound at high temperatures is less than specific heat in Yb compound. Specific heat C_p at 300 K amounts 387.6 J/molK for $Yb_6MoO_{12-\delta}$ and 427.5 J/mol/K for $Lu_6MoO_{12-\delta}$. Both these values are significantly lower than the Dulong-Petit limit of 473.9 J/molK for both compounds.

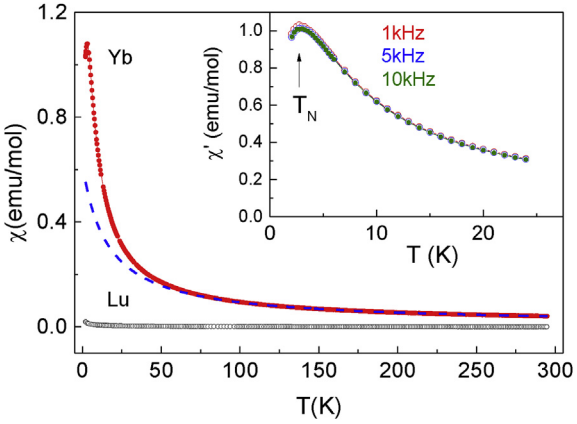

Fig. 3. The temperature dependences of dc magnetic susceptibility χ of $R\bar{3}$ polymorphs of $Yb_6MoO_{12-\delta}$ (upper curve) and $Lu_6MoO_{12-\delta}$ (lower curve). The fitting of χ vs. T dependence for $Yb_6MoO_{12-\delta}$ is shown by dash line. The inset represents the temperature dependences of the in-phase part of *ac* magnetic susceptibility χ′ in $Yb_6MoO_{12-\delta}$ taken at various frequencies.

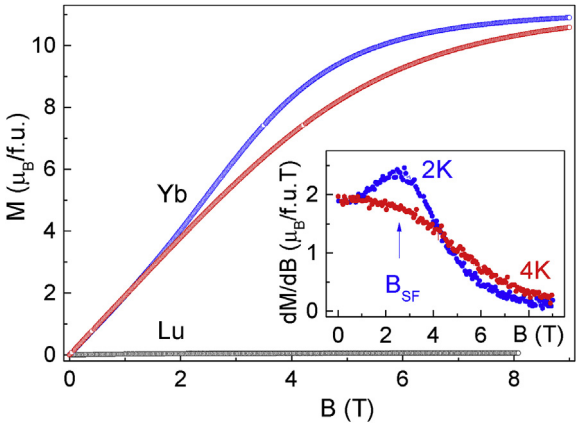

Fig. 4. The field dependences of magnetization M of $R\bar{3}$ polymorphs of $Yb_6MoO_{12-\delta}$ and $Lu_6MoO_{12-\delta}$. The inset represents the dM/dB vs. B curves taken both below and above T_N.

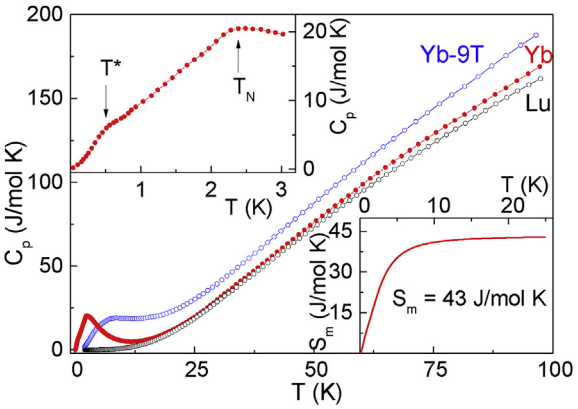

Fig. 5. The temperature dependences of specific heat C_p in $R\bar{3}$ polymorphs of $Yb_6MoO_{12-\delta}$ and $Lu_6MoO_{12-\delta}$. The upper inset represents the ultra-low temperature data down to 100 mK. The lower inset shows the temperature dependence of magnetic entropy in Yb compound.

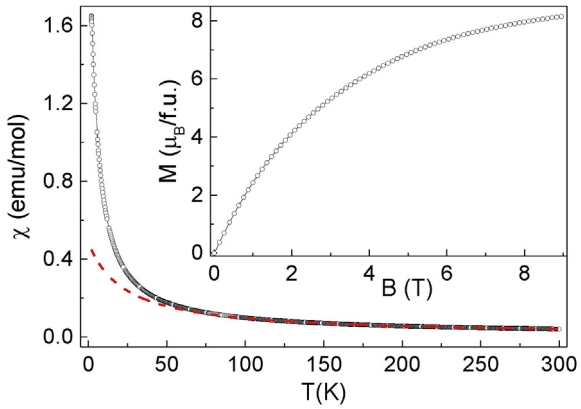

Fig. 7. The temperature dependences of *dc* magnetic susceptibility χ of $Ia\bar{3}$ polymorph of $Yb_6MoO_{12-\delta}$. The fitting curve is shown by dash line. The inset represents the field dependence of magnetization taken at 2 K.

To confirm bulk long-range character of magnetic ordering in $Yb_6MoO_{12-\delta}$, zero-field neutron powder diffraction data were collected at 1.6 K and 10 K, as shown in Fig. 6, i.e. below and above the anomaly observed in the variable temperature magnetic susceptibility and specific heat data. Examination of the data revealed an additional peak in the 1.6 K NPD data, as shown in the inset to Fig. 6. Although, a single peak was not sufficient to determine magnetic structure of the material, nevertheless it unambiguously indicated that $Yb_6MoO_{12-\delta}$ is magnetically ordered at 1.6 K that is consistent with the property measurements.

The temperature dependence of dc magnetic susceptibility χ of $Ia\bar{3}$ polymorph of $Yb_6MoO_{12-\delta}$ is shown in Fig. 7. The treatment of experimental data as described above results in specific chemical formula $Yb^{3+}_{4.3}Yb^{2+}_{1.7}MoO_{11.15}$. The fitting parameters for this compound are $\chi_0 = 7.6 \times 10^{-3}$ emu/mol, $C = 11.0$ emu/molK and $\Theta = -23$ K. The field dependence of magnetization M in $Yb_6MoO_{12-\delta}$ ($Ia\bar{3}$) taken at 2 K is shown in the inset to Fig. 7. This dependence follows the Brillouin function inherent for a paramagnetic state. The whole of available data points to the absence of magnetic order in the temperature range studied.

Despite the fact that the compounds under investigation looks magnetically dense being constituted by both rare-earth and transition metals in a wide temperature range they exhibit purely paramagnetic behaviour. The weakness of magnetism stems from the chemical composition of Ln_6MoO_{12}. At stoichiometry, 4d shell of Mo^{6+} ions is empty while 4f shell of Lu^{3+} ions is full, both being inactive magnetically. Thus, magnetic properties of Lu_6MoO_{12} are due exclusively to deviations from oxygen stoichiometry. The oxygen deficiency results in appearance of reduced Mo^{5+} ions with 4d [1] configuration. These ions are randomly distributed in the structure. This circumstance along with competition of various exchange interactions prevents the formation of long range order in non-stoichiometric $Lu_6MoO_{12-\delta}$.

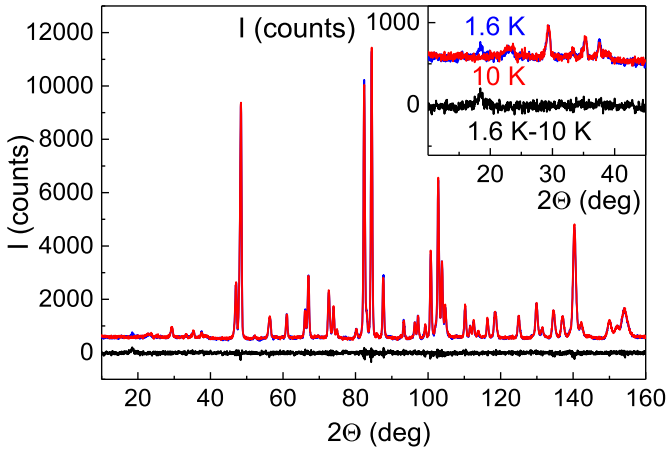

Fig. 6. Neutron powder diffraction data (λ = 2.4395 Å) for $Yb_6MoO_{12-\delta}$ collected at 1.6 K (blue) and 10 K (red), and their difference (black). The inset shows the enlarged low-angle region where an additional magnetic diffraction peak can be seen at 2θ~18°. (For interpretation of the references to colour in this figure legend, the reader is referred to the Web version of this article.)

The only compound which reaches the magnetically ordered state is the rhombohedral modification of $Yb_6MoO_{12-\delta}$ ($R\bar{3}$).This is a surprising result since namely this compound evidences strongest deviation from stoichiometry. The Neel temperature T_N ~2.5 K is close to that in binary compound Yb_2O_3 ($T_N = 2.25$ K) [18]. However, the specific heat anomaly at low temperatures cannot be attributed to the presence of 5.7 wt % of this impurity. Large magnetic entropy release $S_m = 43$ J/molK contradicts to this assumption. The early neutron diffraction study of the magnetic structure in Yb_2O_3 has revealed complex non-collinear arrangement of ytterbium moments incompatible with dipole-dipole interactions. Similarly complex may be the magnetic structure in $Yb_6MoO_{12-\delta}$. Tentatively, the anomaly in specific heat of this compound at $T^* = 0.5$ K may be associated with rearrangement of Yb^{3+} magnetic moments at low temperatures.

Similarly surprising is the absence of magnetic ordering in the cubic modification of $Yb_6MoO_{12-\delta}$ ($Ia\bar{3}$). The deviation from stoichiometry is smaller in this compound. Nevertheless, it remains paramagnetic down to lowest temperatures. It seems, that the absence of the long range magnetic order in $Yb_6MoO_{12-\delta}$ ($Ia\bar{3}$) is associated with mixed occupation of the same crystallographic positions by Yb^{3+} and Mo^{6+} ions.

4. Summary

In conclusion, we undertook first experimental study of thermodynamic properties of several representatives of Ln_6MoO_{12} system. We find that the compounds under study exhibit magnetism largely influenced by deviation from stoichiometry. The only magnetically ordered compound, $Yb_6MoO_{12-\delta}$ ($R\bar{3}$), gives indication on rearrangement of magnetic subsystem at ultra-low temperatures. This is confirmed in low temperature neutron diffraction

measurements.

Acknowledgements

Support from Russian Foundation for Basic Research, grant 17-02-00211, is acknowledged. This work has been supported also by Ministry of Education and Science of the Russian Federation through NUST «MISiS» grant К2-2017-084 and by the Act 211 of the Government of Russia, contracts 02.A03.21.0004, A03.21.0006 and 02.A03.21.0011.

References

[1] H. He, J.D. Bosonetta, K.A. Wheeler, S.P. May, Chem. Commun. 53 (2017) 10120–10123.
[2] H. Kerner-Czeskleba, G. Tourne, Mater. Res. Bull. 13 (1978) 271–278.
[3] J.A. Hodges, P. Bonville, A. Forget, J.P. Sanchez, P. Vulliet, M. Rams, K. Królas, Eur. Phys. J. B 33 (2003) 173–181.
[4] D. Schildhammer, G. Fuhrmann, L. Petschnig, N. Weinberger, H. Schottenberger, H. Huppertz, Dyes Pigments 138 (2017) 90–99.
[5] E.A. Tkatchenko, Proc. SPIE-Int. Soc. Opt. Eng. 3734 (1998) 33–34.
[6] Yu.E. Bogatov, M.G. Safronenko, E.A. Tkachenko, O.V. Sakharova, Russ. J. Inorg. Chem. 42 (1997) 519–522.
[7] J.A. Alonso, F. Rivillas, M.J. Martinez-Lope, V. Pomjakushin, J. Solid State Chem. 177 (2004) 2470–2476.
[8] V.A. Efremov, N.N. Davydova, L.Z. Gokhman, A.A. Evdokimov, V.K. Trunov, Russ. J. Inorg. Chem. 33 (1988) 1732–1738.
[9] E.A. Aitken, S.F. Bartram, E.F. Juenke, Inorg. Chem. 3 (1964) 949–950.
[10] P.H. Hubert, R.A. Paris, C.R. Seances, Acad. Sci. 271 (1970) 1179–1180.
[11] P. Gall, P. Gougeon, J. Solid State Chem. 181 (2008) 1–6.
[12] P. Gall, P. Gougeon, K.V. Ramanujachary, W.H. McCarroll, M. Greenblatt, J. Solid State Chem. 134 (1997) 45–51.
[13] L.F. Schneemeyer, T. Siegrist, T. Besara, M. Lundberg, J. Sun, D.J. Singh, J. Solid State Chem. 227 (2015) 178–185.
[14] A.V. Shlyakhtina, S.N. Savvin, N.V. Lyskov, I.V. Kolbanev, O.K. Karyagina, S.A. Chernyak, L.G. Shcherbakova, P. Nunez, J. Mater. Chem. A 5 (2017) 7618–7630.
[15] K. Momma, F. Izumi, J. Appl. Crystallogr. 44 (2011) 1272–1276.
[16] G.A. Bain, J.F. Berry, J. Chem. Educ. 85 (2008) 532–536.
[17] D.G. Karraker, J. Chem. Phys. 55 (1971) 1084–1086.
[18] R.M. Moon, H.R. Child, W.C. Koehler, L.J. Raubenheimer, J. Appl. Phys. 38 (1967) 1383.